

Signatures of homoclinic motion in quantum chaos

D. A. Włodarczyk^{1,2}, E. Vergini^{1,3}, R. M. Benito⁴ and F. Borondo¹¹Departamento de Química CFI, Universidad Autónoma de Madrid, Cantoblanco, 28049 Madrid (Spain).²Departamento de Física "J. J. Giambiagi", FCEN, UBA,

Pabellón 1, Ciudad Universitaria, 1428 Buenos Aires, Argentina.

³Departamento de Física, Comisión Nacional de Energía Atómica, Av. del Libertador 8250, 1429 Buenos Aires (Argentina).⁴Departamento de Física, E.T.S.I. Agrónomos, Universidad Politécnica de Madrid, 28040 Madrid (Spain).

(Dated: May 22, 2019)

The correspondence in quantum mechanics of classical unstable periodic motion is investigated. Quantum structures localized in the vicinity of periodic orbits appear distributed across a certain width in the corresponding spectrum, that scale with the values of h and the Lyapunov exponent. In this Letter, we numerically study the fluctuations of these widths as a function of the energy in a chaotic system, finding a predominant oscillatory systematic behavior that survives the semiclassical limit. Furthermore, this behavior can be simply explained in terms of the primary homoclinic motion.

PACS numbers: 05.45.Mt, 03.65.Sq, 05.45.(a)

Periodic orbits (POs) and their associated manifolds are invariant classical objects of utmost relevance for the understanding of chaotic dynamical systems [1]. In classical mechanics, the importance of these trajectories, that retrace themselves, was realized very early by Poincaré [2] and others, since, for example, they completely organize the dynamics in the chaotic sea of two dimensional Hamiltonian systems [3]. In quantum mechanics, striking manifestations of these objects have been reported in the literature, in despite of the fact that the notion of trajectory is alien to this theory. For example, POs were used to explain recurrences appearing in the Fourier transform of the quantum density of states [4] and spectra [5], when no other traces of regularity exist, and also the anomalous accumulation of probability density ("scars") that takes place in some high lying eigenvalues of chaotic systems [6]. Actually, before these works appeared, POs were considered by Gutzwiller as the essential ingredient of his celebrated semiclassical theory [7], able to quantize non-integrable systems solely in terms of POs in form.

Being the cornerstone for the description of chaotic dynamical systems, a lot of insight can be gained by considering the following question: How do POs manifest in quantum spectra?

An ideal tool to investigate this issue are non-stationary wave functions highly localized on POs. Recently, a number of methods have been reported in the literature [8, 9, 10, 11], for the systematic calculation of such functions. The overlap with the corresponding eigenstates provides the information on how these structures are embedded in the spectra, and how they appear in the quantum mechanics of the system.

As a first approach, one can start with the minimum possible information concerning the PO, and include only the dynamics in its immediate neighborhood. This corresponds to a tube wavefunction surrounding the PO [12, 13]. The induced dynamics can be followed quan-

tum mechanically by launching a wave packet initially centered at any point on the orbit, $j(0)i$, and computing the autocorrelation function, $C(t) = h(t)j(0)i$. When this is done semiclassically [14, 15] for short times (so that we are in the linear dynamical regime), and the corresponding time domain function Fourier transformed, an envelope in the quasienergy spectrum is obtained. This envelope presents peaks of width $/h$ (h being the PO Lyapunov exponent), at energies corresponding to the Bohr-Sommerfeld (BS) quantization condition on the action plus Maslov contributions. In this way, the envelope defines a restricted range of eigenstates, contributing to each peak with an intensity enhanced by a factor of the order of $(h)^{-1}$ over the random matrix theory [16] predictions.

A better description for the wavefunctions associated to a PO can be obtained by including the (dynamical) information up to times of the order of the Ehrenfest time, then including the hyperbolic structure formed by the corresponding unstable and stable manifolds. In this way, the associated wavefunctions can spread along these dynamically relevant regions of phase space. (See illustration below in Fig. 1). This can be done by a number of methods.

In the first place, Polavieja, Borondo and Benito [8] constructed such type of functions by dynamical average over the dynamics of the PO. Starting from a wave packet, $j(0)i$, well localized in phase space in the vicinity of the PO and allowing the corresponding exact quantum evolution, $j(t)i$, for a time interval of the order of the PO period, the desired wavefunctions are obtained by Fourier transforming $j(t)i$ at suitably quantized values of the energy. These wavefunctions have been shown to have embedded the hyperbolic structure of the PO [17].

Vergini and Carbo [9] provided a precise definition of scar functions by constructing transversally excited resonances along POs at a given BS quantized energies with

minimum dispersion and maximum energy localization. An important point is that their treatment provides an analytical expression for the width of these functions in the energy spectrum, whose leading term is given by,

$$_{sc} = \frac{h}{j \ln h j}; \quad (1)$$

showing that the inclusion of the hyperbolic structure introduces a narrowing factor of $j \ln h_j$ in the width. In this respect, it should be noticed that although this approach incorporate the motion along the manifolds up to the Ehrenfest time, interference effects due to the intersections of the manifolds are not included.

In this Letter, we study the fluctuations with respect to ω_c of the spectral widths corresponding to localized functions calculated in a fully chaotic system. Our results indicate that these fluctuations are surprisingly simple, being essentially governed by the primary homoclinic dynamics associated to the PO, and more importantly that this is a robust conclusion, since they do not seem to vanish as $\hbar \rightarrow 0$. This result is reasonable, since homoclinic orbits constitute the natural extension of the local hyperbolic structure around the PO. Actually, starting from the same consideration, Oзоров and Амелида [18] attempted the calculation of scar states by quantizing homoclinic motions (see also Refs. [19, 20]). There, the homoclinic orbits were thought of as defining a sort of invariant torus that can be approached by series of satellite unstable POs. This swarm of satellite POs was used to compute a reduced summation formula, from which to obtain the corresponding eigenvalues.

As an illustration of these ideas, we present a numerical application to the fully chaotic system consisting of a particle of mass $1/2$ confined in a desymmetrized Bunimovitch stadium billiard, defined by the radius of the circular part, $r = 1$, and the area enclosed, $1 + \pi = 4$. To calculate the corresponding eigenstates, Dirichlet conditions on the stadium boundary and Neumann conditions on the symmetry axes are imposed. We will focus our attention on the dynamics induced by the horizontal P0. The corresponding scar wavefunctions, j_i , are calculated using the method of Ref. [9].

In Fig. 1 we show, as an example, the results for the scar state with wavelength $k_{BS} = 211.665$. This value was obtained from the BS rule, $k_{BS} = (2 = L_H) (n + H = 4)$, where $n = 134$ is the excitation number along the orbit, $L_H = 4$ its length, and $H = 3$ the corresponding Maslov index. In it, all features discussed above are observed. Namely, the Husimi based quantum surface of section [17] spreads along the manifolds structure associated to the horizontal PO, and the state appears in the spectrum distributed among the different eigenstates, j_i , (with weights $j_1 j_2 j_3$) within a given range around the corresponding BS quantized wavelength.

The width of the associated envelope can then be de-

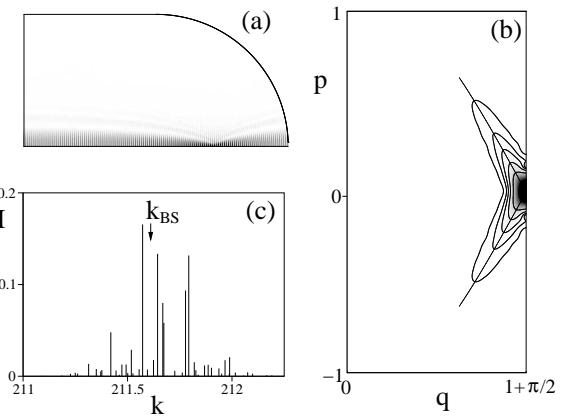


FIG. 1: (a) Configuration space (a), phase space (b), and wavelength spectrum (c) representations of a scar wavefunction along the horizontal periodic orbit of a desymmetrized stadium billiard corresponding to BS wavelength $k_{BS} = 211.665$. The associated unstable and stable manifolds are also plotted in panel (b).

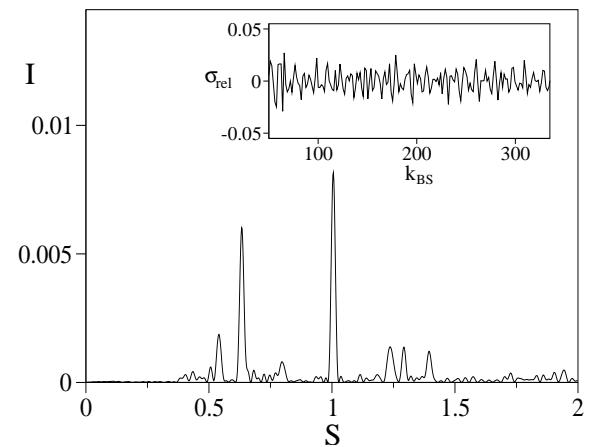


FIG. 2: Relative width for the scar states along the horizontal periodic orbit as a function of the Bohr-Sommerfeld quantized wavelength (inset), and its Fourier transform.

ned as

$$= \frac{s}{x} \frac{1}{(k^2 - k_{BS}^2)^2} : \quad (2)$$

When calculated, this quantity is a decreasing oscillatory function of $k_B s$, that can be more adequately studied by defining its relative variation with respect to the corresponding semiclassical value,

$$\text{rel} \quad \frac{\text{sc}}{\text{sc}} : \quad (3)$$

The corresponding results are shown in the inset to Fig. 2. As can be observed, it exhibit an oscillatory behavior, with an amplitude representing only a small percent of ω_0 . When this signal is Fourier analyzed (see main body of Fig. 2) it is seen to have only two relevant components,

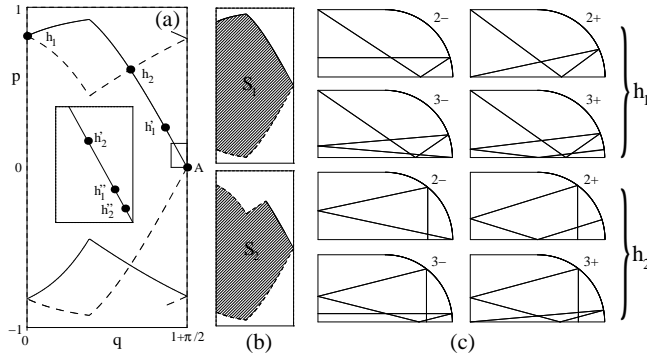


FIG. 3: (a) Phase space portrait in Birkhoff coordinates relevant to our calculations. Label A indicates the position of the fixed point corresponding to the horizontal periodic orbit. The associated unstable and stable manifolds are represented in full and dashed line, respectively. They cross, with different topology, at the primary homoclinic points h_1 and h_2 , which map into h_1^0, h_1^{00}, \dots and h_2^0, h_2^{00}, \dots . (b) Phase space projections of the relevant areas, S_1 and S_2 , defined by the primary homoclinic motion. (c) Satellite periodic orbits converging to the homoclinic points h_1 and h_2 . See text for details.

corresponding to the peaks appearing at values of the action $S = 0.633$ and 1.007 , respectively. (Notice that, in our case, S has units of length since the total linear momentum of the particle has been set equal to one).

To interpret this result, we follow Oзорио де Альмейда [18], and consider only the primary homoclinic motion corresponding to the horizontal PO. There are two topologically distinct types of primary homoclinic points, which appear as the first and second intersections of the associated manifolds. The situation is shown in Fig. 3 (a), where a picture of the relevant phase space, in Birkhoff coordinates, is presented. In it, we have plotted the fixed point corresponding to the horizontal PO (labelled A), and the emanating unstable (full line) and stable (dashed line) manifolds. These manifolds cross (with different topology) at points h_1 and h_2 , and afterwards at sequences h_1^0, h_1^{00}, \dots and h_2^0, h_2^{00}, \dots (and their reflections with respect to $p = 0$), as fixed point A is approached. These infinite sequences of points are the dynamical images of h_1 and h_2 , and define the two primary homoclinic orbits, respectively. This primary homoclinic motion defines two relevant areas in phase space, denoted hereafter as S_1 and S_2 , that are important for the discussions presented below. They are shown as shaded regions in Fig. 3 (b). Furthermore, primary homoclinic orbits accumulate in finite sets of satellite POs with increasingly longer periods, as discussed in Ref. [21]. The first members of these two families, converging to the primary homoclinic orbits are presented in Fig. 3 (c). Accordingly to our notation, based on the number of times that the POs lie over the horizontal path, orbits $2\{$ and $2+$ consist of fixed points near h_1, h_1^0 (or h_2, h_2^0), and their reflections with respect

to $p = 0$; orbits $3\{$ and $3+$ consist of fixed points near h_1, h_1^0, h_1^{00} (or h_2, h_2^0, h_2^{00}), and their reflections; and so on for the longer POs in the family. Moreover, these POs can be grouped in pairs, in such a way that $2\{$ and $2+$ represent the first approximation to the primary homoclinic motion, $3\{$ and $3+$ the second, etc. Actually, it is apparent the increasing relation of these orbits to the horizontal one, since as we progress in the sequence new segments closer and closer to the horizontal axis are incorporated into the trajectory.

Now, the question arises about under which conditions the satellite families of POs reinforce the contribution of the central one. As seen before, the horizontal PO satisfy the BS quantization condition

$$kL_H - \frac{1}{2}h = 2n_H; \quad (4)$$

being n_H an integer. In the same way, the BS condition for orbits 2 , lying twice across the horizontal PO, reads

$$kL_2 - \frac{1}{2}2 = 2n_2; \quad (5)$$

Combining eqs. (4) and (5), a new quantization condition emerges

$$k(L_2 - 2L_H) - \frac{1}{2}(2 - 2H) = 2(n_2 - 2n_H); \quad (6)$$

Proceeding in the same way, we obtain for the next orbits in the hierarchy, lying three times over the horizontal [labelled 3 in Fig. 3 (c)],

$$k(L_3 - 3L_H) - \frac{1}{2}(3 - 3H) = 2(n_3 - 3n_H); \quad (7)$$

and this chain of reasoning can be continued for higher members in the families. The relevant point here is that $L_m \rightarrow L_H$ converges exponentially to $S_{h_1} = 0.631610$ and $S_{h_2} = 1.008858$ for the two families h_1 and h_2 , respectively, as shown in Table I. Moreover, $m \rightarrow H$ is independent of m , and it corresponds to $h_1 = 1$ and $h_2 = 3 = 2$. In this way, we are in the position to assess that all satellite orbits of a given family contribute coherently when two BS quantization rules are simultaneously fulfilled: (a) the quantization of the central (horizontal) orbit [Eq. (4)], and (b) the so-called quantization of the homoclinic torus according to Ref. [18],

$$kS_{h_i} - h_i = 2n_i; \quad i = 1, 2; \quad (8)$$

It should be observed that the values of S_{h_1} and S_{h_2} agree extremely well with those obtained numerically for the position of the two main peaks in the spectrum of Fig. 2. On the other hand, these homoclinic areas correspond in our chosen Poincaré surface of section to the following difference of actions

$$S_{h_i} = L_H - S_i; \quad i = 1, 2; \quad (9)$$

m	\bar{L}_m		$m L_H$
	Fam	ily h_1	
2	0.632273	1.009085	
3	0.631633	1.008868	
4	0.631610	1.008858	
5	0.631610	1.008858	

TABLE I: Asymptotic convergence of \bar{L}_m to $m L_H$ as $m \rightarrow 1$, for families h_1 and h_2 of satellite orbits corresponding to the primary homoclinic motion. To improve the convergence we have averaged the length of orbits $m +$ and $m -$ for the same family [see Fig. 3 (c)].

being S_i the areas indicated in Fig. 3 (b).

This notorious influence of the homoclinic motion in the spectra, and thus in the quantum mechanics of our system, is remarkable, especially, when one takes into account that the homoclinic dynamics is the origin of the chaotic behavior in Hamiltonian systems. The reason for this striking behavior is clear. In the motion connected to this region of phase space there are two components. The first one, close to the primary homoclinic torus (satellite POs), is such that the corresponding trajectories interfere coherently, as it has been shown. The second component, associated to the non-primary homoclinic crosses, gives rise to a more complicated self-intersecting torus. These excursions are much longer and the corresponding interference is much less coherent. Accordingly, its influence in the spectra is very diluted, although they have been shown to be able to fully account for the dynamics of the system (at a very high computational cost) [22]. At this point, it is more efficient to consider the fact that in these long excursions, the trajectories get to distant regions of phase space in which they connect with other short POs (heteroclinic connections). This point has been discussed elsewhere [23].

Finally, let us consider if the influence of the homoclinic motion on rel survives the semiclassical limit $\hbar \rightarrow 0$ ($\hbar \neq 1$ in our units). For this purpose we have performed the following calculation. Starting from the scaled fluctuation curve rel , presented in the inset to Fig. 2, we compute the Fourier transform of the function for increasingly larger intervals of k , $(k_0; k_1)$, keeping fixed the value of the lower limit, k_0 . The results for the peak at S_{h_1} are shown in Fig. 4, where it is seen that the corresponding Fourier intensity divided by $(k)^2$ is an approximately constant function of the length of the interval, $k = k_1 - k_0$. A similar behaviour is obtained for the peak at S_{h_2} . This result implies that $\text{rel}(k_B S)$ is essentially an oscillatory function with frequencies S_{h_1} and S_{h_2} and constant coefficients.

Summarizing, we have studied the fluctuations of the relative widths corresponding to wavefunctions (with

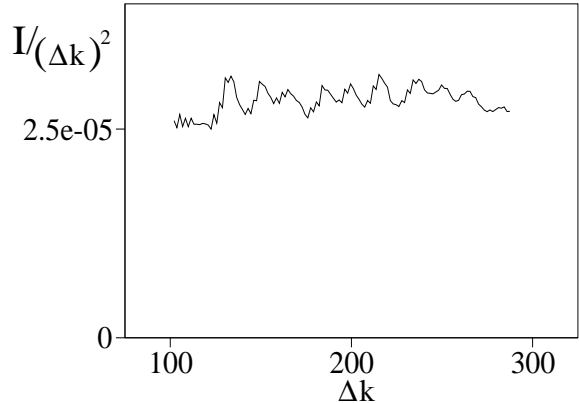


FIG. 4: Intensity of the peak at S_{h_1} divided by $(k)^2$ as a function of k

hyperbolic structure) highly localized in the vicinity of a PO in a classically chaotic system. We show that these magnitudes are clearly controlled by the associated primary homoclinic motion, which thus imprints a clear signature in the quantum spectra of such systems.

This work was supported by MCYT and M CED (Spain) under contracts BFM2000-0437, BQU2003-08212, SAB2000-0340 and SAB2002-022.

E-mail address: fborondo@uam.es

- [1] R. Seydel, *From Equilibrium to Chaos: Practical Bifurcation and Stability Analysis* (Elsevier, Amsterdam, 1988).
- [2] H. Poincaré, *New Methods of Celestial Mechanics*, edited by D. L. Goro (American Institute of Physics, 1993).
- [3] S. Wiggins, *Chaotic Transport in Dynamical Systems* (Springer-Verlag, New York, 1992).
- [4] D. Wintgen, *Phys. Rev. Lett.* 58, 1589 (1987).
- [5] A. H. Olle, G. W. Bush, J. M. Cain, B. Hager, H. Rottke, and K. H. Wrede, *Phys. Rev. Lett.* 56, 2594 (1986).
- [6] E. J. Heller, *Phys. Rev. Lett.* 53, 1515 (1984).
- [7] M. C. Gutzwiller, *Chaos in Classical and Quantum Mechanics* (Springer-Verlag, New York, 1990).
- [8] G. G. de Polavieja, F. Borondo, and R. M. Benito, *Phys. Rev. Lett.* 73, 1613 (1994).
- [9] E. G. Vergini and G. Carlo, *J. Phys. A* 34, 4525 (2001).
- [10] F. Faure, S. Nonnenmacher and D. de Bièvre, *Comm. Math. Phys.* 239, 449 (2003).
- [11] S.-Y. Lee and S. C. Chapman, *Ann. Phys.* 307, 392 (2003).
- [12] E. G. Vergini, *J. Phys. A* 33, 4709 (2000).
- [13] E. G. Vergini and G. Carlo, *J. Phys. A* 33, 4717 (2000).
- [14] E. J. Heller, *Chaos and Quantum Physics* edited by M. J. Giannoni, A. Voros, and J. Zinn-Justin (Elsevier, Amsterdam, 1991).
- [15] L. Kaplan and E. J. Heller, *Ann. Phys. N.Y.* 264, 171 (1998).
- [16] C. E. Porter and R. G. Thomas, *Phys. Rev.* 104, 483 (1956).
- [17] D. A. Wisniacki, F. Borondo, E. Vergini, and R. M. Benito, *Phys. Rev. E* 63, 66220 (2001).

- [18] A .M .O zorio de A lm eida, *Nonlinearity* **2**, 519 (1989).
- [19] M .J.D avis, *J. Phys. Chem.* **92**, 3124 (1988).
- [20] A .A .Zem bekov, F .Borondo, and R .M .Benito, *J. Chem . Phys.* **107**, 7934 (1997).
- [21] G .L .Da Silva R itter, A .M .O zorio de A lm eida, and R .D ouady, *Physica D* **29**, 181 (1987).
- [22] S .Tom sovic and E .J .H eller, *Phys. Rev. Lett.* **47**, 664 (1991).
- [23] D .A .W isniacki, F .Borondo, E .V ergini, and R .M .Benito, *eprint nlin.CD /0311052*.